Ocean Engineering 169 (2018) 110–124

Contents lists available at ScienceDirect

Ocean Engineering

journal homepage: www.elsevier.com/locate/oceaneng

A COLREGs-based obstacle avoidance approach for unmanned surface vehicles

Yanlong Wang[a,*], Xuemin Yu[b,**], Xu Liang[a], Baoan Li[a]

[a] School of Automation Science and Electrical Engineering, Beihang University, Beijing, China
[b] Institute of Information Engineering, Chinese Academy of Sciences, Beijing, China

ARTICLE INFO

Keywords:
Obstacle avoidance
Unmanned surface vehicle
Local path planning
COLREGs
Normal distribution curve

ABSTRACT

This paper reports the preliminary research results of a novel automatic obstacle avoidance approach based on the COLREGs for unmanned surface vehicles (USVs). The approach presented is essentially a path searching-based algorithm called the local normal distribution-based trajectory, which plans viable avoidance trajectories in the presence of both static and dynamic obstacles. The proposed algorithm can generate a COLREGs-compliant suboptimal trajectory based on the bell-shaped curve of normal distribution and extract waypoints for the navigation controller to steer USVs safely. In addition, we discuss three key parameters and present a trajectory replanning strategy to improve the safety and flexibility of our approach. The common overtaking, crossing and head-on collision scenarios are each simulated in experiments. It is shown through simulations that the proposed approach considers multiple factors and can plan paths to avoid obstacles safely and smoothly. A comparison is also made with a reactive path planning algorithm which has been modified to follow the COLREGs.

1. Introduction

Unmanned surface vehicles (USVs) are autonomous marine vessels that can execute multiple tasks in a variety of cluttered marine environments without human supervision (Manley, 2008; Tang et al., 2015). USVs are characterized by small size, high mobility and good hiding capability; they can be used in many marine applications, including oceanography, remote sensing, environmental monitoring, surveying, weapons delivery, mapping and navigation, along with providing communication support for unmanned underwater vehicles and general robotics research (Naeem et al., 2012; Tang et al., 2015; Wang et al., 2018).

Technological development is driving USVs towards “persistent existence”. The future progress of USVs depends on the development of full autonomy, which would enable USVs to work in any unstructured or unpredictable environment without human intervention (Liu et al., 2016). One of the main challenges in enhancing USV autonomy is the simultaneous detection and avoidance of obstacles in either open or confined waters (Campbell et al., 2014). To overcome the obstacle avoidance challenge, hierarchical strategy-based obstacle avoidance approaches, composed of global path planning algorithms and local obstacle avoidance algorithms, have been proposed for USVs (Tang et al., 2015).

Global path planning for USVs is mainly designed to find the optimal global path to avoid static obstacles in a mapped environment. Global path planning can be conducted offline via common path finding heuristic algorithms such as A*, optimization theory such as linear programming, and evolutionary algorithms such as genetic algorithm. Wang et al. (2017) presented a novel path search algorithm for global path planning based on electronic charts and improved A* algorithm. This algorithm can generate safe and reasonable global path for USVs quickly. Kim et al. (2014) proposed a new approach based on Theta* algorithm to create paths in real-time, considering both angular rate and heading angle of USVs. Zhuang et al. (2011) presented a global path search algorithm for USVs based on improved Dijkstra algorithm, where planning time is reduced, and planning precision is improved. Wang et al. (2018) presented a global path search algorithm among multiple task points based on an improved A* algorithm, ant colony optimization and hexagonal grids, which can plan an optimal path to tour multiple task points safely and quickly.

Local obstacle avoidance for USVs is used to avoid static and dynamic obstacles by adopting a timely avoidance manoeuvre in which line-of-sight (LOS) and artificial potential field are widely employed (Campbell et al., 2012). Local obstacle avoidance algorithms are of two types: path searching-based local path planning, which can generate appropriate trajectories or waypoints followed by the vehicle, and the

* Corresponding author.
** Corresponding author.
E-mail addresses: wylloong@163.com (Y. Wang), yuxuemin@iie.ac.cn (X. Yu).

https://doi.org/10.1016/j.oceaneng.2018.09.012
Received 9 February 2018; Received in revised form 8 July 2018; Accepted 5 September 2018
Available online 20 September 2018

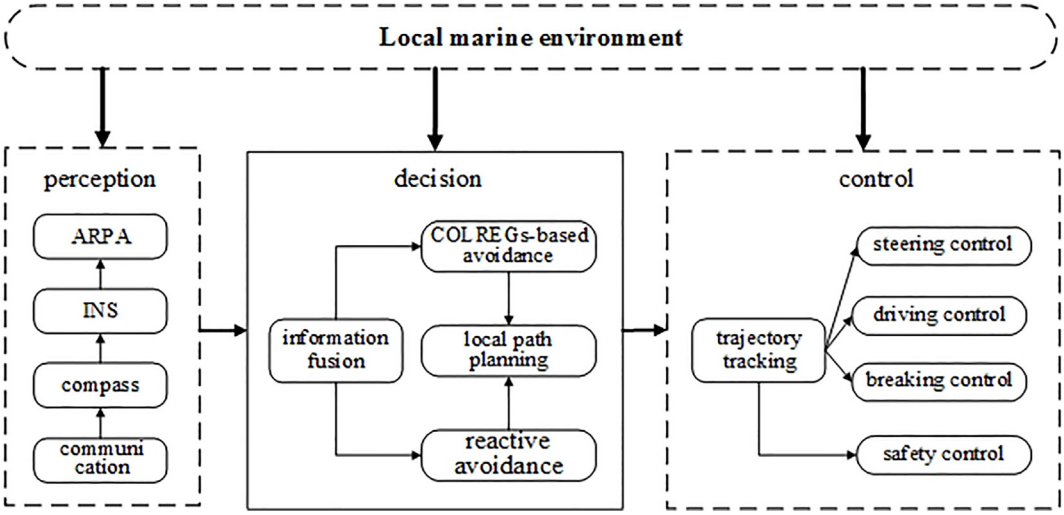

Fig. 1. The architecture diagram of obstacle avoidance.

behaviour-based reactive obstacle avoidance method, which can generate the guidance angle and guidance velocity realized by the navigation controller in real time.

Many researchers make efforts to address the local obstacle avoidance problem over the years. Tang et al. (2012) proposed a near-field reactive static obstacle avoidance method for USVs based on a dynamic window, and the excellent navigation angle, rotational velocity, and translational velocity can be gotten by solving the constraint problem of static obstacles. Zhuang et al. (2013) designed a reactive obstacle avoidance method based on the relative velocity modelling, where the obstacle avoidance of USVs is completed by changing speed and course. Tang et al. (2015) presented a novel general local reactive obstacle avoidance algorithm for high-speed USVs, which is verified by experiments in simulations and sea trials in real marine environments, and the motion of USVs depends on the guidance angle and guidance translational velocity during navigation. Kuwata et al. (2011) put forward a meritorious motion planning approach for USVs in which the Velocity Obstacles (VO) algorithm is adopted to generate a collision-free path while obeying the COLREGS rules. Naeem et al. (2012) adopted a strategy consisting of waypoint guidance by LOS coupled with a manual biasing scheme under COLREGs, and this algorithm is able to generate a non-optimal viable trajectory in the presence of both stationary and dynamic obstacles.

Although many novel algorithms for better real-time implementation of obstacle avoidance in a cluttered environment have been proposed over the years, the local obstacle avoidance problem still limits the wide application of USVs. For example, there are still drawbacks associated with LOS and artificial potential field methods, such as the potential to overshoot and a lack of consideration of the next manoeuvre. Additionally, USVs must behave in a manner that is discernible by other vessels in the vicinity, so the obstacle avoidance approach should integrate marine traffic rules. However, only a few studies have successfully integrated those rules into the obstacle avoidance process, and few obstacle avoidance approaches can simultaneously avoid both static and dynamic obstacles.

Based on the premise that the existing literature does not sufficiently address obstacle avoidance problems and that much effort is still required to optimize these obstacle avoidance approaches, a novel path searching-based algorithm called the local normal distribution-based trajectory (LNDT) is proposed in this paper to address the local obstacle avoidance problem of USVs in complicated encounter situations. This algorithm can generate a suboptimal collision-free path and determine a real-time collision avoidance manoeuvre based on a set of waypoints. The avoidance manoeuvre in the LNDT algorithm includes diverting around static geographical obstacles and avoiding collision with approaching vessels, in compliance with the COLREGs.

The overall scheme of obstacle avoidance is illustrated in Fig. 1. The decision-making module in the dashed frame includes a two-layered distributed architecture of obstacle avoidance; we primarily study the COLREGs-based obstacle avoidance approach.

The remainder of this paper is organized as follows: the next section describes the basic collision avoidance design of USVs. Section 3 presents the LNDT algorithm in detail. Section 4 presents the algorithm flow of the LNDT. Section 5 verifies the algorithm on a local obstacle avoidance simulation platform. Finally, the conclusion and future work are discussed in section 6.

2. Basic obstacle avoidance design

The primary need with regard to obstacle avoidance is increasing autonomy in terms of obstacle detection and appropriate avoidance manoeuvres with minimal or no supervision from a human operator. The obstacle avoidance approach we propose is able to assess collision situations and avoid obstacles automatically by generating trajectories for USVs to minimize their dependency on human intervention, which is a vital element for a fully autonomous surface vehicle.

2.1. COLREGs-based obstacle avoidance rules

Given that there cannot be any verbal communication between the two vessels when a USV takes evasive manoeuvres to avoid an approaching vessel, the USV must take obstacle avoidance measures that are discernible by other vessels in the vicinity. Furthermore, recent statistics show that 60% of casualties at sea are caused by collisions and that 56% of collisions are caused by COLREGs violations (Liu et al., 2016; Campbell et al., 2014). Hence it is necessary for both USV and manned vessels to abide by some pre-defined rules in the course of obstacle avoidance.

The international regulations for preventing collisions at sea (COLREGs), defined by the International Maritime Organization (IMO) in 1972, is designed to maintain a high level of safety at sea. It defines universal and definitive guides for executing standard avoidance manoeuvres, and applies to all vessels upon the high seas and in all waters connected therewith navigable by seagoing vessels (IMO, 1972).

COLREGs are designed to be followed by navigators while operating all types of vessels or watercrafts. Although there is no relevant maritime navigation laws or regulations for USVs, COLREGs rules must be obeyed if USVs sail at sea lawfully. Otherwise, unpredictable or

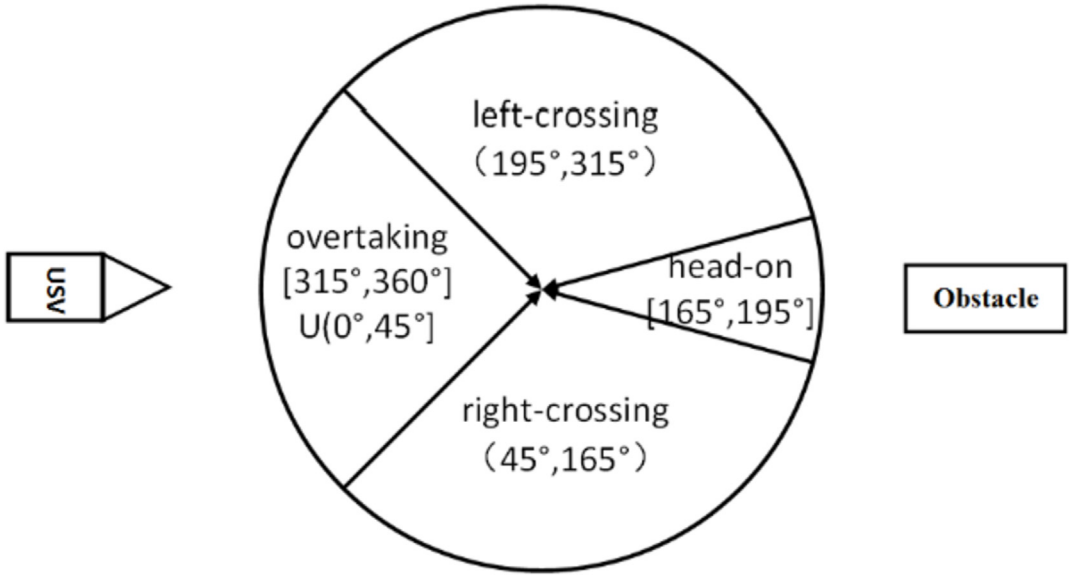

Fig. 2. Schematic of obstacle collision situations.

incorrect avoidance manoeuvres may lead to confusion and potentially catastrophic collisions (Campbell et al., 2012).

The COLREGs, which were written for human operators, are deliberately vague with respect to the angles and zones to which they apply. They thus depend heavily on human common sense and experience in determining both rule applicability and rule execution (Benjamin and Curcio, 2004). Despite the thoroughness of the COLREGs, it is difficult for USVs to understand and comply with them automatically. To apply these rules to USVs, a large amount of human intuition and experience is expected to fill in gaps in the COLREGs.

In order to integrate the COLREGs into the obstacle avoidance approach of USVs, we divide common collision situations into three different behaviours: overtaking, crossing and head-on (Fig. 2). These parameters have been determined through experiments and testing based on the literature and on experts' experience. Setting the course of the USV and the dynamic obstacle at θ_o and θ_t, respectively, the relative course is $\Delta\theta = \theta_o - \theta_t$; we determine the collision situation according to $\Delta\theta$ based on the COLREGs in Fig. 2, with two vehicles at risk of collision (Benjamin and Curcio, 2004; Larson et al., 2008).

To address the three collision situations of overtaking, crossing and head-on, rules 13, 14 and 15 of the COLREGs suggest specific avoidance manoeuvres in each case. We design collision avoidance rules for USVs in accordance with these COLREGs rules, and USVs must abide by these avoidance manoeuvres during the obstacle avoidance process in order not to impede the navigation of other vessels. Specially, according to subparagraph (a) (ii) of rule 17 in COLREGs, USVs should take action to avoid collision alone, as soon as it becomes apparent to her that the vessel required to keep out of the way is not taking appropriate action (e.g. the other Give-way vessel required to keep out of the way is not altering her course to starboard in left-crossing situation). The main COLREGs-based collision avoidance rules for USVs and schematics are listed in Table 1 (Benjamin and Curcio, 2004; International Maritime Organization, 1972). The detailed obstacle avoidance manoeuvres are discussed in the following sections.

2.2. Obstacle avoidance architecture

When USVs operate in complex marine environments, local path planning requires reliable obstacle perception and obstacle avoidance. Cameras, Automatic Radar Plotting Aids (ARPAs), compasses and Global Positioning System (GPS) devices are widely employed for environment perception and obstacle detection on most USVs. In general, the geographic position and motion state of USV are provided by on-board sensors, while the ARPA radar sensor can measure the proximity of an object, determine its velocity relative to the USV and predict its future velocity and position (Campbell et al., 2012). In this paper, we apply a customized ARPA radar to perceive the local environment; it is capable of detecting obstacles and calculating the closest point of approach (DCPA) and the time to the closest point of approach (TCPA) with other vessels by extrapolating other vessels' position in time.

Collision risk assessment is vital before an USV makes any obstacle avoidance decisions. The risk assessment is mainly determined by DCPA, TCPA, vessel size and the preset safety distance, which together reflect collision possibility and the degree of collision risk (Li and Pang, 2013). The lower the DCPA, the greater danger of collision; the lower the TCPA, the more urgent it is to take obstacle avoidance action. If the DCPA is less than a preset threshold distance in future time, the USV is in danger of collision with other vessel(s).

Using multi-sensor fusion technology, this paper presents a dynamic two-dimensional real-time map that classifies collision scenarios and builds behaviour constraints for obstacle avoidance according to the COLREGs. The overall scheme for obstacle avoidance is illustrated in Fig. 1, which shows a two-layered distributed architecture to solve the problem of obstacle avoidance. The distributed architecture consisting of two concentric circles is shown in Fig. 3, with the local environment divided into two parts – the COLREGs-based region and the emergency region; the grey circles in them represent obstacles.

The COLREGs-based region with radius *Ra* lies inside the ARPA radar detection area. Once other obstacles enter this region, the collision risk assessment method will assess the collision situation based on DCPA and TCPA parameters. Provided that an obstacle poses a collision risk to the USV, the USV should anticipate local path planning in compliance with the COLREGs and then follow the planned path, based on the LNDT algorithm, to avoid the obstacle.

The planned path generated using the LNDT algorithm can avoid collision with the majority of vehicles in the COLREGs-based region. However, if an encounter situation is not covered by the COLREGs, as when a high-speed vessel makes a turn towards port instead of starboard in a head-on scenario, reflexive avoidance actions must be taken to ensure that a collision does not occur in the emergency region. If other obstacles come into the emergency region with radius *Re* at any

Table 1
Particular manoeuvres in various obstacle avoidance situations.

Rule No	Situations	Relative rules in COLREGs	Schematics
Rule 13	Overtaking	Any vessel overtaking any other shall keep out of the way of the vessel being overtaken	
Rule 14	Head-on Situation	When two power-driven vessels are meeting on reciprocal or nearly reciprocal courses so as to involve risk of collision each shall alter her course to starboard so that each shall pass on the port side of the other.	
Rule 15	Crossing Situation	When two power-driven vessels are crossing so as to involve risk of collision, the vessel which has the other on her own starboard side shall keep out of the way and shall, if the circumstances of the case admit, avoid crossing ahead of the other vessel.	
Rule 16	Action by Give-way Vessel	Every vessel which is directed by these rules to keep out of the way of another vessel shall, so far as possible, take early and substantial action to keep well clear.	
Rule 17	Action by Stand-on Vessel	Where by any of these rules one of two vessels is to keep out of the way the other shall keep her course and speed.	

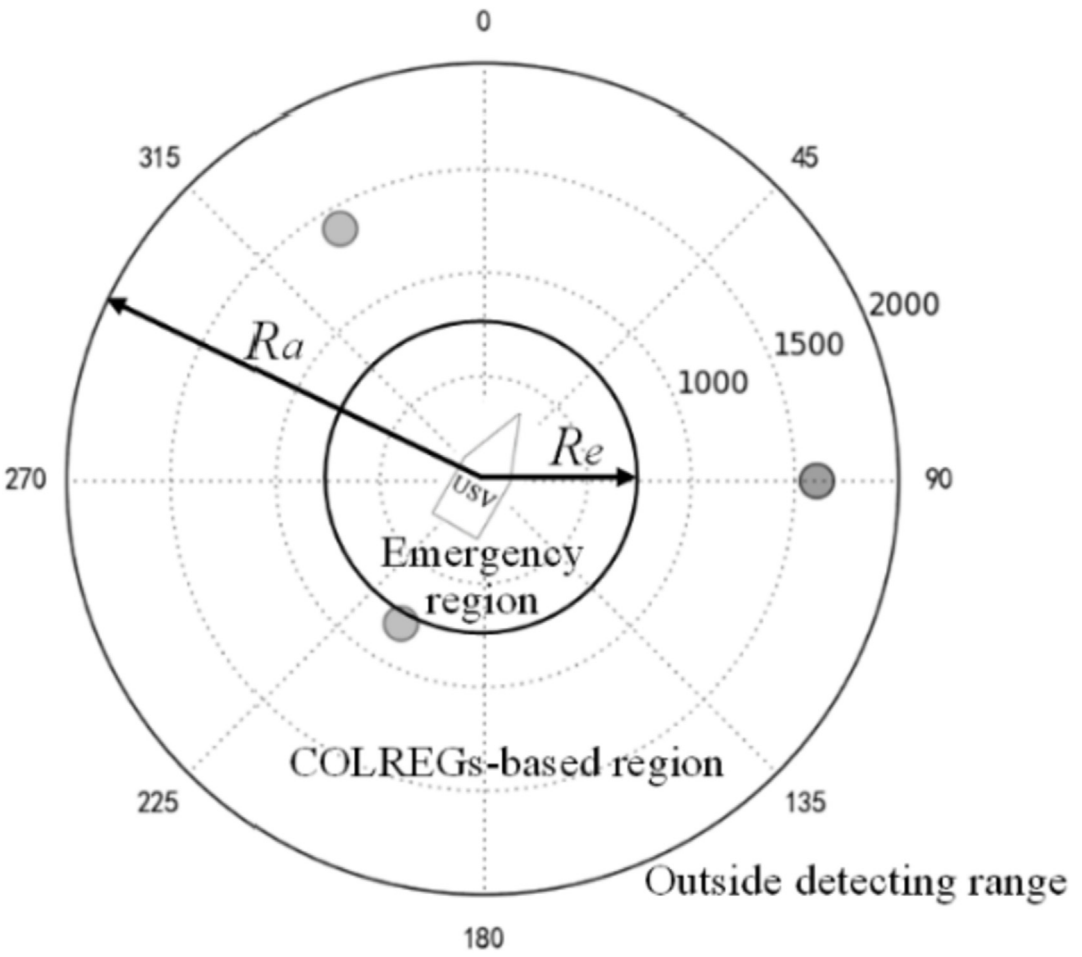

Fig. 3. Schematic of the two-layered environment map.

time, the USV should take reflexive action to avoid collision at any cost where safety is paramount, even not following the COLREGs. The artificial potential field and behaviour-based voting methods are widely employed in the emergency region; they can avoid short-range obstacles by modifying the throttle and steering commands in real time (Campbell et al., 2012; Larson et al., 2008). Thus, we focus primarily on deliberative path planning that complies with the COLREGs in the COLREGs-based region.

By combining the kinematic characteristics of USVs and the two-layered distributed architecture, the proposed obstacle avoidance approach can plan a suboptimal local obstacle avoidance trajectory based on the LNDT algorithm when an obstacle poses a danger to USV in the COLREGs-based region. In addition, our approach downloads waypoints extracted from the trajectory to the navigation controller, which can then steer the USV to follow that trajectory and so evade obstacles.

2.3. Obstacle avoidance behaviour assessment

Many researchers have tried to address the obstacle avoidance problem and presented various approaches from different perspectives. Given that there is currently no effective method to assess the performance of these approaches, it is necessary to establish a scientific and impartial obstacle avoidance behaviour assessment (OABA) method to optimize these approaches to the greatest extent possible.

Relying on the practical experience of navigators, this section proposes six evaluation indicators: obstacle avoidance time, path safety, path length, path smoothness, path deviation and the closest distance for OABA. These six indicators describe obstacle avoidance performance from different perspectives, which helps to compare and analyse the existing obstacle avoidance algorithms.

Obstacle avoidance time: This refers to the total time required by an obstacle avoidance process: the less time spent on obstacle avoidance, the better performance of the obstacle avoidance algorithm. The indicator T can be expressed as follows:

$$T = t_e - t_s \tag{1}$$

where t_s is the start time of obstacle avoidance and t_e is the end of obstacle avoidance.

Path safety: This refers to the average distance between the USV and the obstacle *OBS* during the obstacle avoidance process: the greater the average distance, the higher the safety of navigation. The indicator *PSA* can be expressed as follows:

$$PSA = \frac{\sum_{t_s}^{t_e} \left\| USV - OBS \right\|}{t_e - t_s} \tag{2}$$

where the $\| \ \|$ operator is used to calculate the relative distance between *USV* and *OBS*.

Path length: This refers to the sailing distance in the course of obstacle avoidance: the shorter the total distance, the better the obstacle avoidance performance. The indicator L can be expressed as follows:

$$L = \sum_{t_s}^{t_e} \left\| P_{t+1} - P_t \right\| \tag{3}$$

where P_t is the geographical coordinate of the USV at moment t.

Path smoothness: This can be evaluated by the sum of course changes during the obstacle avoidance process: the greater the total of course changes, the less smooth the obstacle avoidance trajectory. The indicator *PSM* can be expressed as follows:

$$PSM = \sum_{t_s}^{t_e} |\theta_{t+1} - \theta_t| \tag{4}$$

where θ_t is the course of USV at moment t.

Path deviation: This is evaluated by the average deviation distance of the USV from the global path during the obstacle avoidance process. The indicator *PDE* can be expressed as follows:

$$PDE = \frac{\sum_{t_s}^{t_e} |D_{devi}(t)|}{t_e - t_s} \tag{5}$$

where $D_{devi}(t)$ is the deviation distance from the global path at moment t.

Closest distance: This refers to the closest distance between the USV and the obstacle during the obstacle avoidance process. The indicator *LCLD* can be expressed as follows:

$$LCLD = \min(\|P_t - OBS\|) \tag{6}$$

CABA is the foundation of obstacle avoidance approaches. In this section, we propose six evaluation indicators to realize CABA and thus help to compare and improve the obstacle avoidance of USVs.

3. Local normal distribution-based trajectory algorithm

In general, global path planning for USVs can avoid static obstacles like islands and lighthouses featured in electronic charts (Wang et al., 2017, 2018), but a USV may also encounter hazardous unmarked static obstacles and dynamic obstacles in its vicinity, such as vessels and floaters, when following a global planned path. If these obstacles seriously threaten the USV's navigation safety, the USV is required to deviate temporarily from its global path to avoid a collision. As to the set of global waypoints that the USV is to follow, each waypoint is assumed to have a specific purpose for its creation, so the USV also must return to the global path as soon as possible after completing any obstacle avoidance actions.

In this paper, the maximum detecting distance of sensors is set at 2 km; with few dangerous obstacles within the COLREGs-based region in open waters, it is also understood that the USV only needs to avoid a single obstacle in practice. Thus, we mainly discuss obstacle avoidance approaches for a single obstacle in open waters and propose the LNDT path searching-based obstacle avoidance algorithm, which plans a suboptimal local obstacle avoidance trajectory that follows the COLREGs.

3.1. Local normal distribution-based trajectory

USVs have a limited perception range for near-field obstacles, so they should take collision avoidance measures as soon as possible after perceiving collision risk. Furthermore, USVs are required to take collision avoidance measures that are discernible by nearby vessels. The avoidance manoeuvres of USVs thus need to consider these factors: COLREGs-based obstacle avoidance rules, the safe distance of approach, the safe distance of passing, the distance of last action (DLA), the kinematic characteristics of USV, the avoidance time and the time needed to return to the global trajectory.

In this paper, we construct the LNDT, a local normal distribution-based trajectory algorithm with variable parameters, that is essentially a path searching-based algorithm. The LNDT algorithm abides strictly by the COLREGs and considers the necessary factors listed above to complete behaviour planning for avoiding obstacles. The trajectory generated by the LNDT algorithm is composed of three approximately semi-circular arcs; it is similar to the bell shape found in normal distribution. We extract a set of waypoints with timestamps from the trajectory so that the USV can complete obstacle avoidance by changing its velocity and course.

Normal distributions are important in statistics and are often used in the natural and social sciences to represent real-valued random variables whose distributions are not known (Casella and Berger, 2002). The LNDT algorithm establishes its mathematical modelling of obstacle

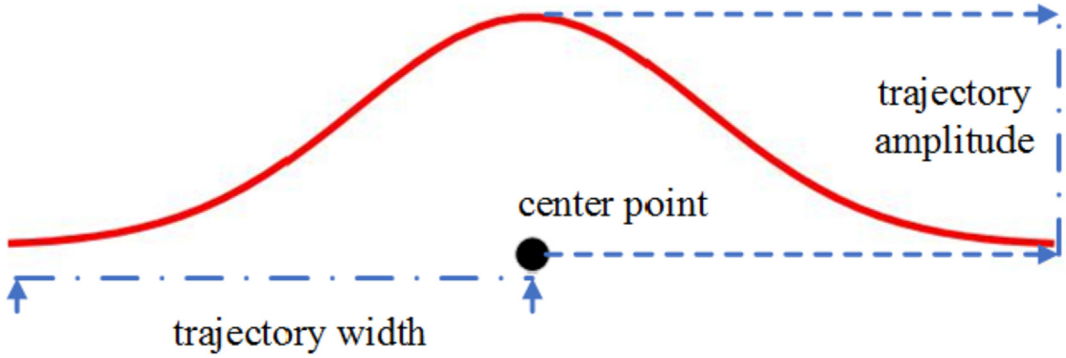

Fig. 4. Schematic of the local obstacle avoidance trajectory.

avoidance based on the bell curve of normal distribution and improves normal distribution to meet obstacle avoidance demands.

The simplified expression of the obstacle avoidance trajectory along the X-axis based on the bell curve of normal distribution is defined in Eq. (7), where the parameters σ and μ no longer have statistical meaning:

$$f(x) = \mathrm{A}\cdot\exp\left(-\frac{(x-\mu)^2}{2\sigma^2}\right) \qquad x \in (\mu - 3\sigma, \mu + 3\sigma) \tag{7}$$

As Fig. 4 shows, the centre point μ that can dynamically translate the trajectory is related mainly to the DCPA and TCPA parameters. The trajectory amplitude parameter A, which determines the height of the trajectory, is an important parameter in ensuring navigation safety. The trajectory width parameter σ, which determines the width of the trajectory, is related to the DLA and the relative velocity vector of the two vessels. The parameter x is related to the start and end times of obstacle avoidance; its value generally ranges from μ−3σ to μ + 3σ.

Eq. (7) can easily generate an obstacle avoidance trajectory along the X-axis in the Mercator coordinate system. Any planned path of obstacle avoidance should extend along the global path, which means that the expression of the obstacle avoidance trajectory in Eq. (7) cannot meet the actual situation when the global path is not parallel to the X-axis. Fortunately, the trajectory along the X-axis can be converted to the trajectory along the global path through the following translational and rotational steps:

1. We take the coordinate origin as the centre point and generate the trajectory along the X-axis according to the determined parameters.
2. The generated trajectory is then rotated anticlockwise around the coordinate origin in the direction of the global path.
3. The rotated trajectory is translated to the centre point of the trajectory, thus making it consistent with the target trajectory generated along the global path.

In step 2, for any point (x, y) in the generated trajectory, we can obtain a new point (x_1, y_1) defined in Eq. (8) after rotating an angle θ anticlockwise around a fixed point (r_x, r_y).

$$\begin{cases} x_1 = (x - r_x)\cos(\theta) - (y - r_y)\sin(\theta) + r_x \\ y_1 = (x - r_x)\sin(\theta) - (y - r_y)\cos(\theta) + r_y \end{cases} \tag{8}$$

where θ is the angle by which the X-axis rotates anticlockwise in the direction of the global path.

Given that the nature of the trajectory will not change after rotation and translation, we take the trajectory generated along the X-axis as the object of discussion only when it relates to the nature of the trajectory, even though the global path is not parallel to the X-axis.

After generating the planned trajectory, the LNDT algorithm extracts a set of waypoints from the trajectory at regular intervals Δt and downloads these waypoints into the navigation controller to steer the USV safely. The extracted waypoint $W(t_i) = \{H(t_i), T(t_i), P(t_i)\}$ contains the parameters of the geographic position $P(t_i)$, the expected arrival time $T(t_i)$ and the expected course $H(t_i)$, which are defined in Eq. (9). When the USV arrives at any waypoint, it navigates to the next waypoint sequentially.

$$\begin{cases} \|P(t_{i+1}) - P(t_i)\| = v_{USV}\cdot\Delta t \\ T(t_{i+1}) - T(t_i) = \Delta t \\ H(t_{i+1}) = \mathit{Trajectory\ slope} \approx \arctan\left(\frac{P(t_{i+1}).y - P(t_i).y}{P(t_{i+1}).x - P(t_i).x}\right) \end{cases} \tag{9}$$

The USV then follows the desired trajectory depending on the guidance angle ${\theta^t}_{guidance}$ and the guidance translational velocity ${v^t}_{guidance}$, both given by the navigation controller. The navigation controller, who is responsible for velocity control, course control and trajectory tracking, can steer the USV to track the planned trajectory, where ${\theta^t}_{guidance}$ and ${v^t}_{guidance}$ are defined in Eq. (10) according to the set of waypoints.

$$\begin{cases} {v^t}_{guidance} = \frac{\|USV - P(t_{i+1})\|}{T(t_{i+1}) - t_{current}} \\ {\theta^t}_{guidance} = \arctan\left(\frac{P(t_{i+1}).y - USV.y}{P(t_{i+1}).x - USV.x}\right) \end{cases} \tag{10}$$

Below, we discuss the characteristics of the trajectory generated by

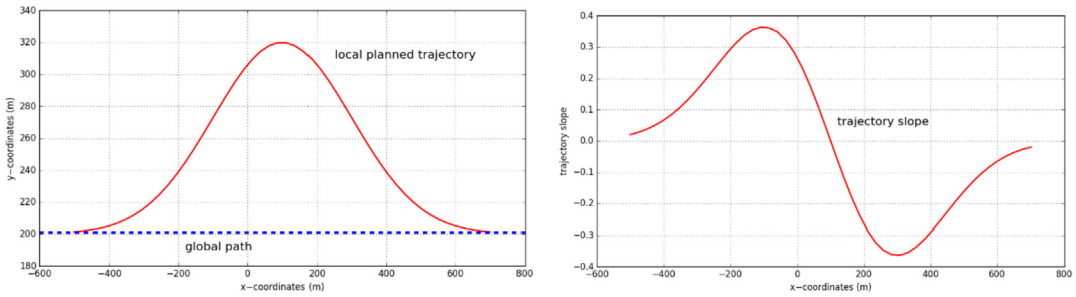

Fig. 5. Characteristics of the obstacle avoidance trajectory.

the LNDT algorithm to prove that the trajectory has the ability to deal with the several constraints mentioned above during the obstacle avoidance process.

The LNDT algorithm has the advantage of a simple formula, wide application, practicality and flexibility. For example, the trajectory amplitude, trajectory width and centre point can all be dynamically adjusted to express various bell shapes in different obstacle avoidance scenarios. We suppose that the parameters of trajectory width, centre point and trajectory amplitude are 200, (100, 200) and 120, respectively; the final path generated is shown in Fig. 5.

Fig. 5(a) shows that the planned trajectory extends along the global path and is composed of three semi-circular arcs; the obstacle avoidance process can be completed by steering the rudder three times in an ideal situation, which simplifies the control strategy without repeating rudder behaviour. In the early stage of obstacle avoidance, the beginning segment of the obstacle avoidance trajectory approximately overlaps the global path, which leads the USV to deviate smoothly from the global path and follow the planned trajectory without large fluctuations. In the middle segment, the USV deviates from the global path significantly to ensure a safe relative distance between it and the obstacle. The last segment of the trajectory coincides with the global path, which leads the USV to return to the global path after completing the obstacle avoidance. As we can see, the LNDT algorithm takes into account path smoothness, the DLA, the avoidance time and the reorientation request. In addition, we analyse the first derivative of the trajectory in Fig. 5 to study the heading of the USV as it follows the trajectory.

As Fig. 5 shows, the overall obstacle avoidance trajectory is relatively smooth, and there are no sharp turns in the course of obstacle avoidance; its curvature is continuous with little rotational velocity, which meshes easily with the kinematic characteristics of the USV.

Finally, the LNDT algorithm can quickly generate a customized obstacle avoidance trajectory with rapid calculation before obstacle avoidance, and the off-board monitor can clearly discern the next step in USV behaviour from the planned trajectory, so the LNDT algorithm following the COLREGs is more advanced than the traditional behaviour-based reactive method in certain ways.

3.2. Key parameters of the LNDT

There are three key parameters in Eq. (7) – trajectory width σ, centre point μ and trajectory height A – which determine the bell shape of the obstacle avoidance trajectory. The three parameters are all given physical meanings associated with DLA, DCPA and safe passing distance parameters. Additionally, the navigation safety of the USV during the obstacle avoidance process is closely related to these parameters. For example, the greater the DLA requests, the earlier beginning of obstacle avoidance, so DLA and σ are positively related. In addition, μ is located on the global path and is closely related to the most dangerous point, and the USV has to deviate sufficiently from the global path to ensure safety as it nears the dangerous point.

This section focuses on the procedure for determining the centre point, trajectory width and trajectory amplitude parameters based on the two-dimensional environment map. We usually determine trajectory width and centre point first and then calculate the optimal trajectory amplitude according to the collision situation.

We take the right-crossing scenario as an example to discuss the trajectory parameter determination procedure, with the relative course $\Delta\theta$ between the two vessels in the range of 45°–165°. We introduce the ship coordinate system to simplify the procedure, in which the direction of the global path is taken as the Y-axis, and the velocity and the course of USV are v_u and θ_u, respectively, with the geographic position (x_u, y_u). Similarly, the velocity and course of obstacle vessel are v_o and θ_o, respectively, with the geographic position point (x_o, y_o).

If the DCPA parameter in a right-crossing scenario is less than the preset safety passing distance, the USV is in danger of collision with obstacles unless it undertakes evasive behaviour. In the ship coordinate system, we can extrapolate the point (x_A, y_A) in the global path closest to the obstacle at the TCPA in Eq. (11), where θ_Δ is the azimuth of the obstacle relative to the USV:

$$\begin{cases} x_A = x_u + v_u \cdot \sin\theta_u \cdot Tcpa + Dcpa \cdot \sin\theta_\Delta \\ y_A = y_u + v_u \cdot \cos\theta_u \cdot Tcpa + Dcpa \cdot \cos\theta_\Delta \end{cases} \tag{11}$$

In addition, the intersection point (x_B, y_B) of the obstacle's track with the global path in the ship coordinate system is as defined in Eq. (12):

$$\begin{cases} x_B = 0 \\ y_B = \begin{cases} y_o + \left|\frac{x_o}{\tan\theta_o}\right|, & \theta_o \in (0,90] \cup (270,360) \\ y_o - \left|\frac{x_o}{\tan\theta_o}\right|, & \theta_o \in (90,270) \end{cases} \end{cases} \tag{12}$$

The trajectory width σ must meet the requirements of obstacle avoidance time: the smaller the relative course angle, the longer the duration of the obstacle avoidance process in a right-crossing scenario, which means that σ needs to be longer. As a result, the relationship between σ and $\Delta\theta$ in the right-crossing scenario is established as in Eq. (13), where C_σ is positively correlated with DLA and k_σ is the regulation parameter:

$$\begin{cases} \sigma = (k_\sigma \cdot |\cos\theta_\Delta| + 1) \cdot C_\sigma, & \theta_\Delta \in (45,90] \\ \sigma = C_\sigma, & \theta_\Delta \in (90,165) \end{cases} \tag{13}$$

We have navigation experience of obstacle avoidance in a right-crossing scenario, as discussed below. In Fig. 6, the two vessels are represented as white vessels at the TCPA and as black vessels after the obstacle vessel crosses the global path; it is clear that the speed component along the global path is less than the original speed of the USV when it follows the planned trajectory. If we take the closest point in Eq. (11) as the centre point of the trajectory, the USV is usually still in the first half of its planned trajectory at the TCPA shown in Fig. 6.

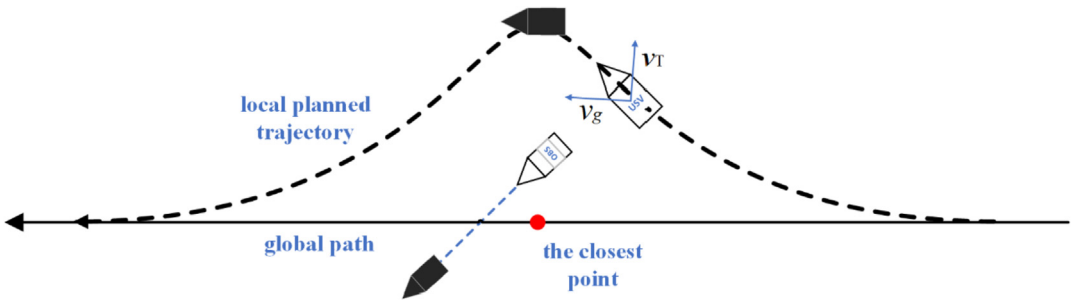

Fig. 6. Diagram of obstacle avoidance process.

In this situation, the obstacle vessel will soon cross the global path if it has not yet crossed the global path at the TCPA. So, the beginning of obstacle avoidance action can be delayed slightly to make it possible for the USV to deviate farthest from the global path when the obstacle is passing through the global path, which makes the trajectory amplitude optimal and improves the efficiency of the planned path. The delay time is positively correlated with the relative course, and the correct moment to begin obstacle avoidance is determined largely by regulating the centre point when the trajectory width is determined, so the regulated centre point (μ_x, μ_y) located in the global path is given by:

$$\begin{cases} \mu_x = k_\mu \cdot |\cos \theta_\Delta| \cdot x_A + (1 - k_\mu \cdot |\cos \theta_\Delta|) \cdot x_B \\ \mu_y = k_\mu \cdot |\cos \theta_\Delta| \cdot y_A + (1 - k_\mu \cdot |\cos \theta_\Delta|) \cdot y_B \end{cases} \tag{14}$$

where k_μ is a positive real parameter whose value determines the relative importance of (x_A, y_A) versus (x_B, y_B).

Similarly, if the obstacle has crossed the global path at the TCPA, the starting time of obstacle avoidance can be slightly advanced, and the regulated centre point (μ_x, μ_y) located in the global path is given by:

$$\begin{cases} \mu_x = (1 - k_\mu \cdot |\cos \theta_\Delta|) \cdot x_A + k_\mu \cdot |\cos \theta_\Delta| \cdot x_B \\ \mu_y = (1 - k_\mu \cdot |\cos \theta_\Delta|) \cdot y_A + k_\mu \cdot |\cos \theta_\Delta| \cdot y_B \end{cases} \tag{15}$$

After determining the centre point and trajectory width, we can calculate the optimal trajectory amplitude A to make the local planned trajectory shorter, smoother and effective in terms of navigation safety. The expression of the obstacle avoidance trajectory can be expressed as in Eq. (16) when the centre point and trajectory width are determined.

$$C(y) = A \cdot \exp\left(-\frac{(y-\mu)^2}{2\sigma^2}\right) \tag{16}$$

The first derivative of Eq. (16) can be expressed as Eq. (17), which is directly related to the heading of the USV when following the trajectory.

$$C'(y) = -\frac{(y-\mu) \cdot A}{\sigma^2} \cdot \exp\left(-\frac{(y-\mu)^2}{2\sigma^2}\right) \tag{17}$$

Supposing that the start time of obstacle avoidance is T and the motion state of the obstacle remains unchanged in the right-crossing situation, we can calculate the position $(x_u + x(t), y_u + y(t))$ of the USV when it follows the planned trajectory at $T + t$ moment, according to the sailing distance $L(y)$ in Eq. (18).

$$L(y) = \int_{\mu_y - 3\sigma}^{y} \sqrt{1 + C'(y)^2}\, dy = v_\mu \cdot t \tag{18}$$

At $T + t$ moment, the position of the obstacle is $(x_o + v_o \cdot \sin \theta_o \cdot t, y_o + v_o \cdot \cos \theta_o \cdot t)$, so the relative distance $D(t)$ of them is given by:

$$D(t) = \sqrt{(x_u + x_u(t) - x_o - v_o \cdot sin\ \theta_o \cdot t)^2 + (y_u + y_u(t) - y_o - v_o \cdot cos\ \theta_o \cdot t)^2} \tag{19}$$

The safe navigation of USVs requires that they maintain the safe relative distance $D(t) \geq D_{safe}$, where D_{safe} is the preset threshold distance, which is related to ship size, navigation accuracy and safe passing distance. $D(t)$ is related to the three key trajectory parameters, so the optimal parameter A_{opt} can be defined as in Eq. (20) when the centre point and trajectory width are determined:

$$A_{opt} = \min_A D(t) \geq D_{safe} \tag{20}$$

Similarly, we can determine the three key parameters of other collision scenarios according to the above procedure, and the parameters in Table 2 can be dynamically regulated according to collision scenarios. With these parameters, the LNDT algorithm can quickly generate suboptimal trajectories that satisfy the COLREGs and consider DLA, the safe approach distance and other factors; it can avoid obstacles and mesh with the kinematic characteristics of USV while ensuring safe sailing.

3.3. Trajectory replanning

Given the kinematic characteristics of vessels and experience drawn from actual navigation cases, we note that a ship's inertia is relatively large, especially with large-sized vessels, whose velocity and heading change slowly. Furthermore, the COLREGs stipulate that the Stand-on vessel is to maintain its course and speed (IMO, 1972). Therefore, the sections above assume that both the velocity and the course of obstacles remain essentially unchanged. Nevertheless, there are some extreme conditions that can cause the obstacles' motion to change sharply, which may result in a collision risk for the USV even as it still follows the planned trajectory. In this situation, it is necessary to replan the obstacle avoidance trajectory to ensure the safety of USV.

When the USV follows a trajectory, its current heading has a time-varying nature that approximates the slope of the current segment of its trajectory. Due to the unstable heading, ARPA radar cannot accurately assess the DCPA and TCPA parameters. Therefore, we need to devise a method to evaluate the closest distance between two vessels in the future when the USV follows the planned trajectory.

Li and Pang (2013) established a relative motion model of vessels and discussed DCPA and TCPA calculation methods (Fiorini and Shiller, 1998). Based on the relative motion model, we propose a waypoint prediction method to calculate the closest distance $D\min$ between two vessels with unstable headings in future time.

The waypoint prediction method can estimate $D\min$ according to the relative motion model when the USV begins to leave one waypoint for the next waypoint. Taking the USV's movement from waypoint A to waypoint B as an example, we can extrapolate the position, velocity and heading of the obstacle vessel at waypoint A, while the position, velocity and heading of the USV at waypoint A can be calculated from the set of waypoints extracted from the trajectory; we can then predict their closest distance according to the motion model without iteration when the USV departs waypoint A for waypoint B. Similarly, we can repeat

Table 2
Key parameters of the LNDT in different collision scenarios.

situation	centre point	trajectory width	trajectory amplitude
crossing	Obstacle has not crossed the global path at TCPA moment: $\begin{cases} \mu_x = k_\mu \cdot \lvert\cos \theta_\Delta\rvert \cdot x_A + (1 - k_\mu \cdot \lvert\cos \theta_\Delta\rvert) \cdot x_B \\ \mu_y = k_\mu \cdot \lvert\cos \theta_\Delta\rvert \cdot y_A + (1 - k_\mu \cdot \lvert\cos \theta_\Delta\rvert) \cdot y_B \end{cases}$ Obstacle has crossed the global path at TCPA moment: $\begin{cases} \mu_x = (1 - k_\mu \cdot \lvert\cos \theta_\Delta\rvert) \cdot x_A + k_\mu \cdot \lvert\cos \theta_\Delta\rvert \cdot x_B \\ \mu_y = (1 - k_\mu \cdot \lvert\cos \theta_\Delta\rvert) \cdot y_A + k_\mu \cdot \lvert\cos \theta_\Delta\rvert \cdot y_B \end{cases}$	$\begin{cases} \sigma = (k_\sigma \cdot \lvert\cos \theta_\Delta\rvert + 1) \cdot C_\sigma, & \theta_\Delta \in (45,90] \\ \sigma = C_\sigma, & \theta_\Delta \in (90,165) \end{cases}$	Eq. (20)
head-on overtaking	$\begin{cases} \mu_x = \frac{x_A + x_B}{2} \\ \mu_y = \frac{y_A + y_B}{2} \end{cases}$	$\sigma = C_\sigma$ $\sigma = k \cdot \frac{v_o}{v_\mu} \cdot (1 + \lvert\cos \theta_\Delta\rvert) \cdot C_\sigma$	

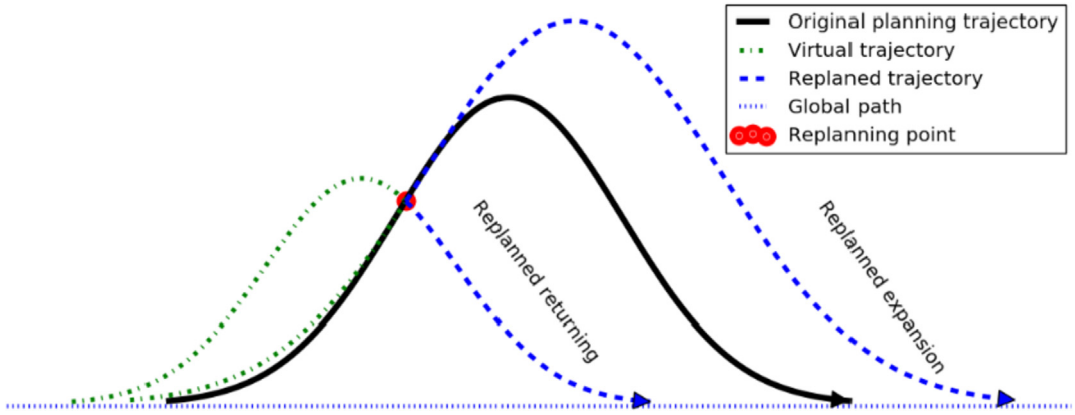

Fig. 7. Two kinds of trajectory replanning strategies.

the above steps to calculate the closest distance among waypoints at a future time. By using the waypoint as the prediction unit, this method has the advantages of small computational amounts and real time; it is superior to the time iteration prediction method.

If the predicted closest distance is less than the safe distance, the USV fails to follow the trajectory due to harsh marine conditions or the local obstacle avoidance trajectory cannot guarantee navigation safety when the motion of the obstacle changes dramatically, the obstacle avoidance trajectory needs to be replanned in order to avoid collision.

While there are several reasons for local path replanning, strategies for replanning generally fall into one of two categories: in a replanned returning trajectory, the USV returns to global path early when there is no collision risk, and the generated trajectory is essentially the second half of a complete obstacle avoidance trajectory, as Fig. 7 shows. The other is a replanned expansion trajectory, in which the USV deviates even farther from the global path, as Fig. 7 shows, and the trajectory amplitude usually increases in response to the current collision situation.

The replanned trajectory is part of the complete obstacle avoidance trajectory generated by the LNDT algorithm. Therefore, the methods of parameter determination and waypoint extraction are similar to the LNDT algorithm and need not be discussed in detail again.

4. Algorithm flow

The architecture chart of obstacle avoidance approach is shown in Fig. 1, where the flow of LNDT algorithm is shown in Table 3.

Table 3
Pseudocode of LNDT.

```
Initial OA=False, t=0; /*OA is obstacle avoidance flag*/
Construct two-dimensional environment map;
while (USV is not reaching the destination)
   Update environment map based on multi-sensor fusion technology;
   if (COLREGs-based region has obstacles and OA=False):
      if (DCPA < Threshold Distance and TCPA < Threshold Time ):
         Set OA as True;
         Calculate trajectory parameters based on Table 2;
         Output: planned trajectory and the set of waypoints based on (7) and (9);
      end if
   else if (OA=True):
      Calculate D_min based on waypoint prediction method;
         if ( D_min < Preset Threshold Distance):
            Calculate trajectory parameters based on Table 2;
            Output: replanned trajectory and waypoints based on (7) and (9);
         end if
         if (USV has completed obstacle avoidance):
            Set OA as False;
         end if
   end if
   if (USV reaches target waypoint P_next ):
      Set target waypoint as P_next+1 ;
   end if
   t=t+1;
end while
End
```

Table 4
Simulation parameters.

Simulation parameter	Value
Simulation cycle	0.1 s
Radius of COLREGs-based region	2000 m
Radius of emergency region	150 m
Minimum safe distance	200 m
Circle-of-acceptance	10 m
maximum sensor detecting distance	2000 m

5. Experimental analyses

The LNDT algorithm is able to generate viable trajectories in the presence of either a stationary or a dynamic obstacle. In order to verify its practicality and reliability, the overtaking, crossing and head-on collision scenarios are each simulated in an obstacle avoidance simulation system. Besides, a comparison is also made with a behaviour-based reactive obstacle avoidance method called biased-LOS, which can generate COLREGs-compliant manoeuvres by line-of-sight coupled with a manual biasing scheme (Naeem et al., 2012).

5.1. Obstacle avoidance simulation system

The obstacle avoidance simulation system allows concurrent development of algorithms and corresponding software, reducing the time required to build a complete solution (Braunl et al., 2006). The system is composed of six simulation modules: on-board sensors, vessel digital simulation, obstacle perception, navigation control, visual simulation and monitoring. These modules can simulate the entire local obstacle avoidance process, including the movement of USVs and obstacles, the dynamic environment perspective, obstacle avoidance and data transmission and processing. With the help of the simulation system, we can verify the LNDT algorithm and compare it with other obstacle avoidance algorithms, which is an enormous advantage in assessing and improving obstacle avoidance approaches for USVs. The parameters used in the simulation system are presented in Table 4.

The typical USV simulated in this paper is approximately 7 m long and 2 m wide with an operating speed of 12 knots (see Fig. 8). The USV is configured by mounting one main aft thruster and one rudder, which produce only two distinct inputs – propulsion force and yaw moment – but its hydrodynamic and dynamic properties are quite complex and difficult to determine accurately. However, obstacle avoidance simulation does not require accurate vessel model parameters. Therefore, we can make some assumptions for the USV in order to simplify its modelling in our simulation system. For example, the rotational velocity model of the USV is reduced to a first-order Nomoto model.

Table 5
Waypoint coordinates for the obstacles avoidance simulation.

ID	WP_0	WP_1	WP_2	WP_3	WP_4
X(m)	0	1600	300	−2300	−5765
Y(m)	0	1600	3032	4532	2532

The following three assumptions are made in the simulation system: all vehicles comply with the COLREGs, the Stand-on vessel maintains its current velocity during the obstacle avoidance process and disturbances from the marine environment (e.g. currents and waves) are negligible.

To verify the capacity of the LNDT algorithm to deal with the problem of obstacle avoidance, a closed-loop path is designed for the experiment; the global waypoints to be reached are listed in Table 5. In the simulation, the USV launches at the origin waypoint WP_0, visits all waypoints and finally returns to WP_0.

5.2. Static obstacle avoidance simulation

As shown in Fig. 9, a single static obstacle is located near the global path as the USV departs from WP_0 and navigates toward WP_1, involving the USV in a possible collision risk with the static obstacle. The on-board ARPA radar detects the obstacle, which can be regarded as a circle with a radius, after expansion, of 100 m with centre geographic position of (800, 1050). Evidently, the USV has a danger of collision in this situation, as the DCPA is only 77 m, which is less than the preset safe distance. Therefore, our obstacle avoidance approach generates a local obstacle avoidance trajectory based on the LNDT algorithm, and guides the USV to bypass the obstacle. Fig. 9 shows the obstacle avoidance track through the two waypoints in chronological order.

Fig. 8. An actual USV during sea trials.

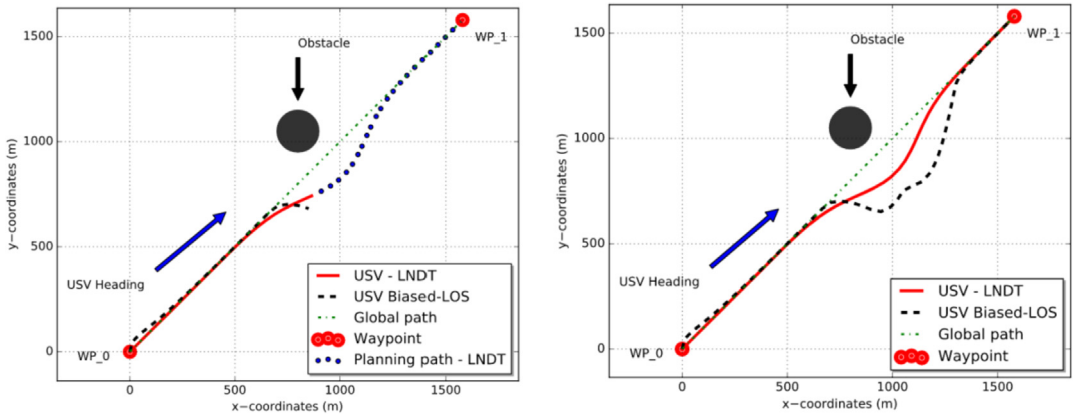

Fig. 9. Track diagram of static obstacle avoidance.

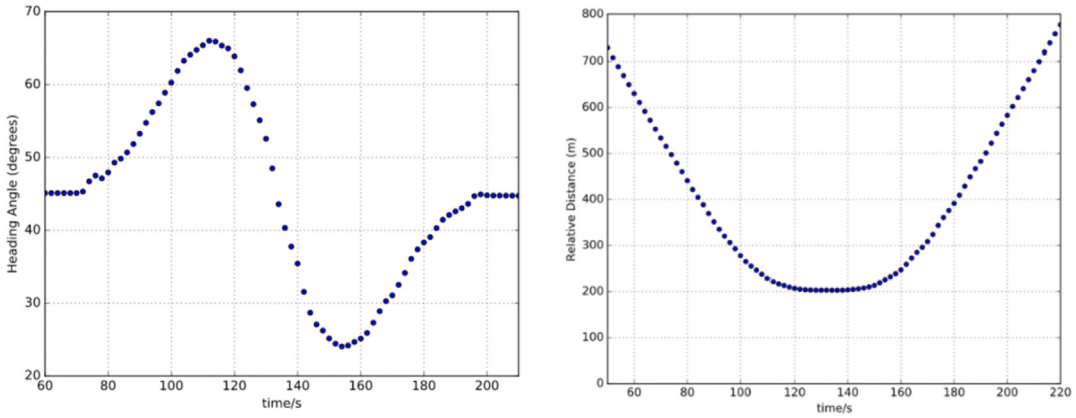

Fig. 10. Local static obstacle avoidance performance of the LNDT.

Fig. 10(a) and (b) show the schematics of the heading angle and relative distance, respectively, as the USV follows the obstacle avoidance trajectory. The relative distance between them remains large enough to keep navigation safe, and the heading changes are continuous and smooth. In addition, the maximum angular velocity is 1.9°/s in the course of obstacle avoidance, which is within the kinematic constraints of the USV.

LOS guidance and its variations are still the simplest and most popular guidance procedures in use today (Campbell et al., 2012). Therefore, we compare the LNDT algorithm with the biased-LOS technique proposed in an existing paper (Naeem et al., 2012). In the biased-LOS approach, we suppose the circle-of-rejection (COR) and circle-of-acceptance (COA) to be 400 m and 50 m, respectively, in the simulation, with the bias angle set at 75° according to existing research and practical applications. The biased-LOS approach can complete obstacle avoidance by changing the USV's speed and course, but it is clearly not optimal because it simply emulates human behaviour without integrating the several factors outlined above.

The sailing track used by the biased-LOS approach during obstacle avoidance is shown in Fig. 9. It is noted that there are chattering phenomena at the COR margin, and the USV returns to the global path slowly after completing the obstacle avoidance process. Fig. 11 illustrates the heading angle and angular velocity of the biased-LOS approach, as tracked by the controller during obstacle avoidance. The

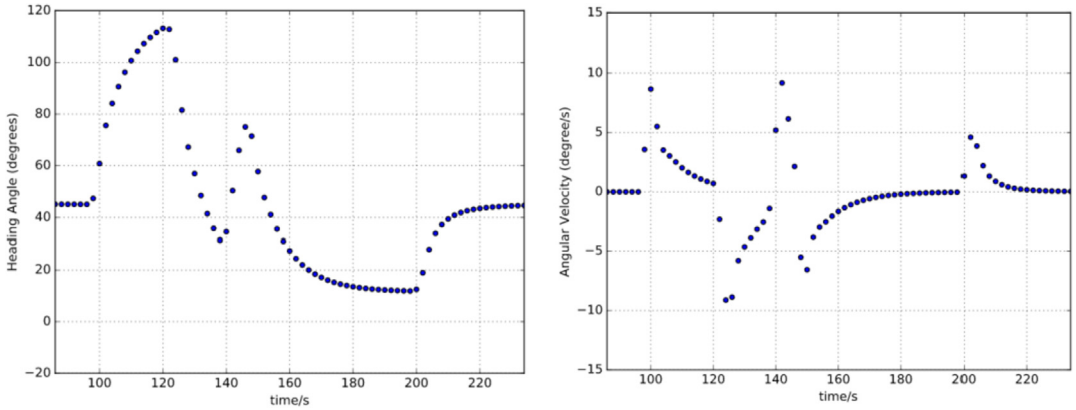

Fig. 11. Local obstacle avoidance performance in a biased-LOS approach.

Table 6
Behaviour evaluation indicators of static obstacle avoidance.

	T	*LCLD*	*PSA*	*L*	*PSM*	*PDE*
LNDT	130s	202.82 m	416.78 m	1302.71 m	130.39°	136.59 m
biased-LOS	128s	250.32 m	465.84 m	1279.81 m	338.52°	125.98 m

results show that the USV heading changes dramatically and that the maximum angular velocity almost reaches the steering limit.

As Fig. 9 shows, the overall trajectory of the LNDT algorithm is much smoother and shorter than the biased-LOS method; their respective behaviour evaluation indicators mentioned in section 2 are presented in Table 6. Although both algorithms can successfully avoid the static obstacle in this situation and thus ensure safe navigation, the simulation results show that the LNDT algorithm is better than the biased-LOS algorithm in safety, feasibility and predictability during the static obstacle avoidance process.

5.3. The dynamic obstacle avoidance simulation

This section simulates common dynamic obstacle avoidance processes in four encounter scenarios to verify the performance of the LNDT algorithm. In addition, we simulate a local path replanning situation supposing that the movement of the obstacle changes during the obstacle avoidance process.

As Fig. 12 shows, a power-driven vessel intends to cross ahead of the USV, which poses a right-crossing collision scenario as the USV navigates from WP_1 to WP_2 in this simulation. The COLREGs stipulate that the USV, as the Give-way vessel, should take early and substantial action to stay out of the way of another vessel; the key parameters of generating the trajectory according to Table 2 are provided in Table 7.

The simulation results are depicted in the following figures, which show that the USV stays out of the way of the obstacle vessel. The sailing tracks of the two vessels in Fig. 12 show that the USV alters its course to starboard and passes by the stern of the obstacle vessel, thus avoiding crossing ahead of the obstacle vessel.

The heading angle and relative distance diagrams of the LNDT algorithm and biased-LOS method are shown in Fig. 13, and their evaluation indicators are presented in Table 8. The results in Fig. 13 and Table 8 demonstrate that the closest distance during obstacle avoidance using a biased-LOS approach is 154 m, which is less than the safe distance, and that the heading of the USV changes dramatically in that method; by contrast, LNDT algorithms can avoid the dynamic obstacle safely, quickly and smoothly. It is clear that the LNDT algorithm, with its smooth trajectory and low angular velocity, performs better than the biased-LOS approach.

Table 7
Parameters of the obstacle avoidance trajectory.

Parameters	Value
Centre point	(1017, 2241)
Trajectory width	200 m
Trajectory amplitude	316 m
Target heading	317.8°

Next, the USV meets a vessel as it navigates from WP_2 to WP_3, and the two vessels are on nearly reciprocal courses, indicating the risk of a head-on collision. The sailing tracks of both vessels are shown in Fig. 14, where the USV alters its course to starboard so that each vessel will pass on the port side of the other, following the COLREGs rules. The results in Fig. 14 demonstrate that the biased-LOS method does not avoid obstacles safely, as its closest distance is less than the safe distance, and the USV deviates too far from the global path. It is clear that the LNDT algorithm with its smooth trajectory is better than biased-LOS method in safety, stability, predictability and deviation distance during the obstacle avoidance process. Due to space limitations, detailed data during the obstacle avoidance process will not be discussed below.

When the USV navigates from WP_3 to WP_4, it intends to overtake a vessel with a velocity less than that of the USV. The sailing tracks of both vessels in this overtaking collision situation are shown in Fig. 15, where the USV alters its course to port and deviates from the global path for some time, in accordance with the COLREGs, so that it can stay out of the way of the vessel being overtaken. Although both algorithms successfully overtake the obstacle vessel, the simulation results in Fig. 15 show that the LNDT algorithm is better than the biased-LOS approach in safety, feasibility, predictability and deviation distance during the obstacle avoidance process.

Although the LNDT algorithm is primarily designed for a single obstacle, it also has a limited capacity to avoid multiple obstacles in the vicinity, and we simulate a complex situation to verify this ability. While the USV navigates from WP_4 back to the origin (WP_0), three power-driven vessels (i.e. V_0, V_1 and V_2) with similar courses intend to cross ahead of the USV, posing a complex right-crossing collision scenario for the USV. We also simulate an additional trajectory replanning situation that supposes that the movement of V_1 changes during the obstacle avoidance process. We consider the three crossing vessels together so that an obstacle avoidance trajectory can be generated by the LNDT algorithm. The velocity of V_1 is 10 m/s in the beginning; however, it decelerates rapidly to 3 m/s when approaching V_0, and the waypoint prediction method forecasts that the USV may be in danger of collision with the obstacle if the USV continues to follow its original trajectory.

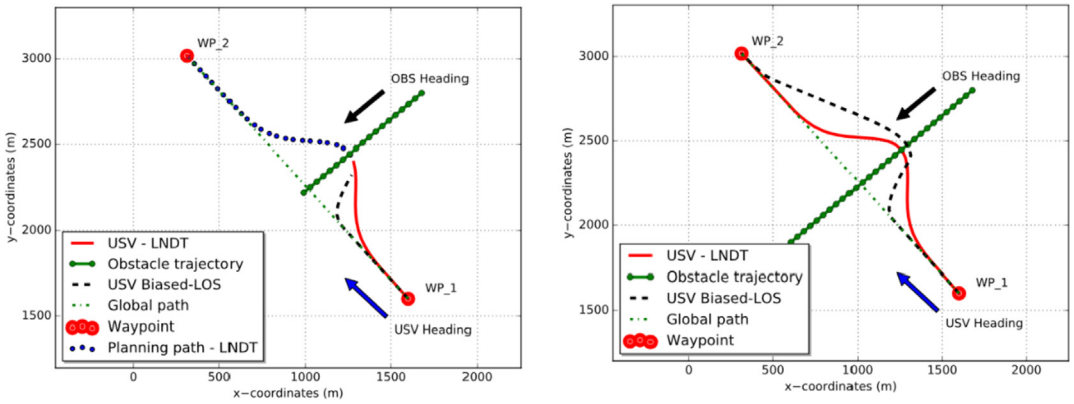

Fig. 12. Track diagram in a right-crossing scenario.

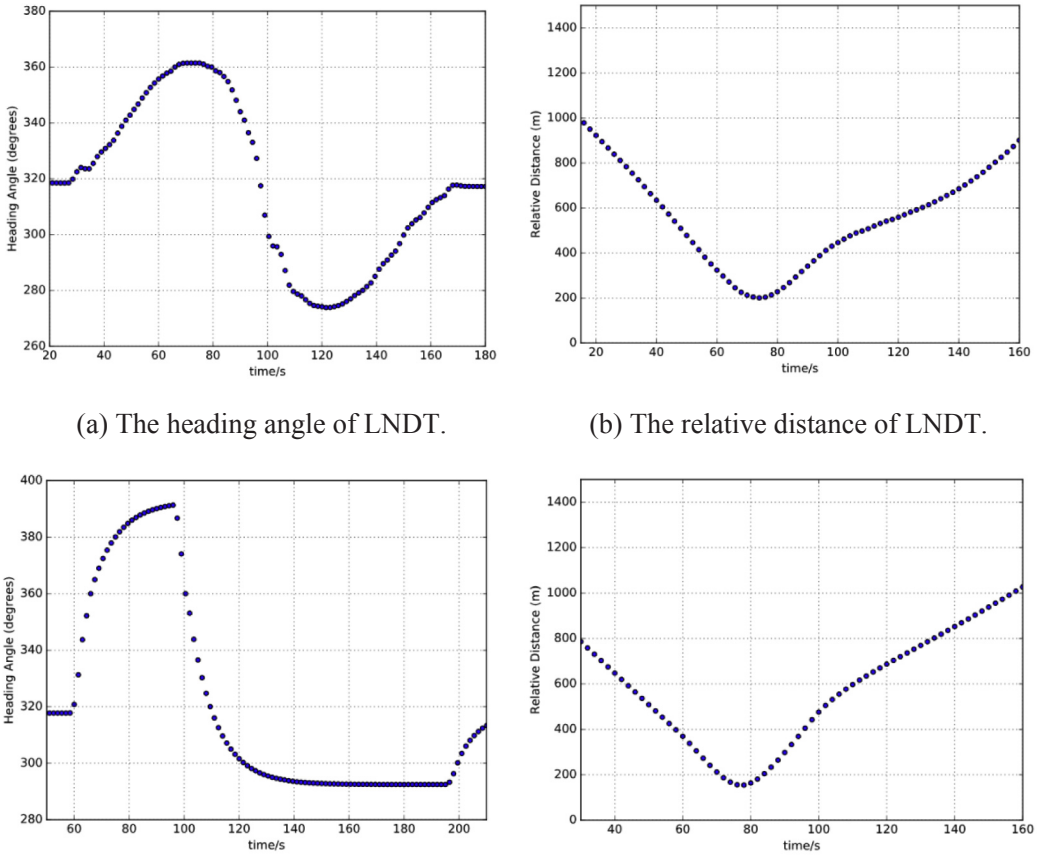

(a) The heading angle of LNDT. (b) The relative distance of LNDT.

(c) The heading angle of LOS. (d) The relative distance of LOS.

Fig. 13. Local obstacle avoidance performance diagram in a right-crossing scenario.

Table 8
Parameters of the obstacle avoidance trajectory in a right-crossing scenario.

	T	*LCLD*	*PSA*	*L*	*PSM*	*PDE*
LNDT	140s	200.72 m	539.19 m	1397.44 m	214.42°	136.59 m
biased-LOS	146s	154.17 m	768.38 m	1459.89 m	227.64°	192.49 m

Under this circumstance, a replanned trajectory is generated by regulating trajectory parameters to deviate significantly from the global path, so the USV can successfully complete obstacle avoidance even though the movement of obstacles has altered. The obstacle avoidance trajectory and performance are shown in Fig. 16, which demonstrates that the LNDT algorithm can take multiple obstacles into consideration and replan the obstacle avoidance trajectory.

Simulation experiments have been carried out both for static and dynamic obstacles. The obstacle avoidance approach we have proposed here – the LNDT – can generate a smooth, viable trajectory that follows the COLREGs and maintains a safe distance from obstacles. The LNDT algorithm considers DLA and meshes with the kinematic characteristics of USV; it can replan the obstacle avoidance trajectory to ensure navigation safety when the movement of obstacles changes. A comparison is also made with a biased-LOS approach, and the LNDT algorithm is

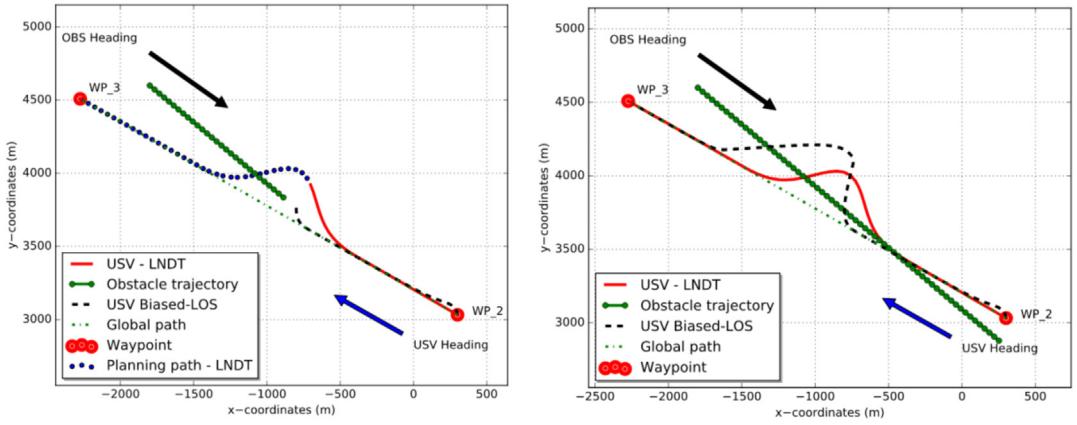

Fig. 14. Track diagram in a head-on scenario.

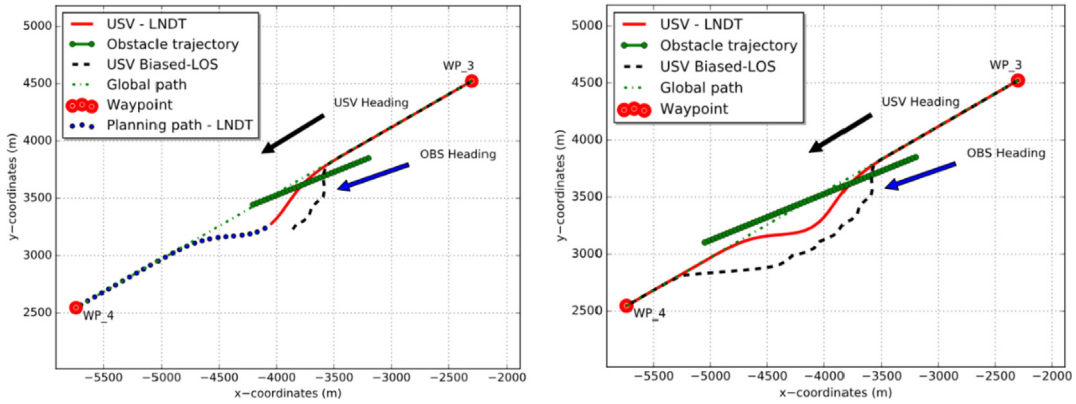

Fig. 15. Track diagram in an overtaking scenario.

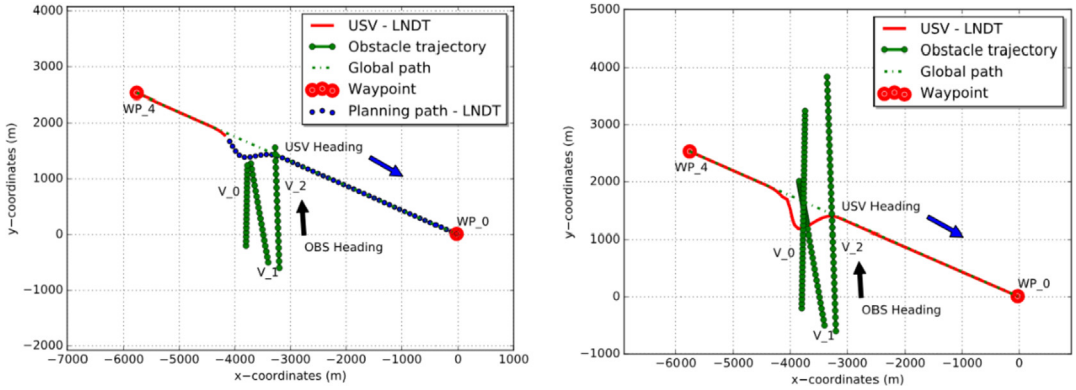

Fig. 16. Track diagram of a complex situation.

demonstrably better in safety, feasibility, predictability and deviation distance.

6. Conclusion

This paper has presented preliminary research results on the development of an obstacle avoidance approach for USVs. According to the COLREGs as defined by the IMO, we describe COLREGs-based collision avoidance rules for USVs that involve relative course parameter. We then propose a novel general obstacle avoidance algorithm called the LNDT for USVs, which can generate viable trajectories in compliance with the COLREGs, based on the bell shape of normal distribution. The highlight here is that the LNDT algorithm integrates multiple factors – the COLREGs, the kinematic characteristics of USVs and DLA – so as to provide realistic trajectories that can be closely followed by USVs. In addition, we have discussed the three key parameters of the LNDT and present a trajectory replanning strategy to improve the safety and flexibility of obstacle avoidance. In the simulation, the capacities of the LNDT were verified in four typical obstacle scenarios. The results demonstrate that the LNDT can indeed guide USVs in realizing safe navigation in the presence of both static and dynamic obstacles. Compared with the biased-LOS approach, the LNDT has better performance in safety, predictability and trajectory smoothness.

In the paper, we focus on the design of a suboptimal obstacle avoidance algorithm for USVs, where the LNDT algorithm is primarily used for a single obstacle. However, the LNDT algorithm has only been verified by simulations. Therefore, we need to research the multi-obstacle avoidance problem, and the LNDT algorithm needs validation in real marine environments.

Acknowledgments

The authors would like to thanks to School of Automation Science and Electrical Engineering at Beihang University, China for allowing the use of USV model for this study.

References

Benjamin, M.R., Curcio, J.A., 2004. COLREGS-based navigation of autonomous marine vehicles. In: Autonomous Underwater Vehicles, 2004 IEEE/OES, pp. 32–39.
Braunl, T., Boeing, A., Gonzalez, L., Koestler, A., Nguyen, M., 2006. Design, modelling and simulation of an autonomous underwater vehicle. Int. J. Veh. Aut. Syst. 4 (2–4), 106–121.
Campbell, S., Abu-Tair, M., Naeem, W., 2014. An automatic COLREGs-compliant obstacle avoidance system for an unmanned surface vehicle. Proc. IME M J. Eng. Marit. Environ. 228 (2), 108–121.
Campbell, S., Naeem, W., Irwin, G.W., 2012. A review on improving the autonomy of unmanned surface vehicles through intelligent collision avoidance manoeuvres. Annu. Rev. Contr. 36 (2), 267–283.
Casella, G., Berger, R.L., 2002. Statistical Inference, vol. 2 Duxbury, Pacific Grove, CA.
Fiorini, P., Shiller, Z., 1998. Motion planning in dynamic environments using velocity obstacles. Int. J. Robot Res. 17 (7), 760–772.
International Maritime Organization, 1972. Convention on the international regulations for preventing collisions at sea. https://treaties.un.org/doc/Publication/UNTS/Volume%201050/volume-1050-I-15824-English.pdf, Accessed date: 30 January 2018.
Kim, H., Kim, D., Shin, J.U., Kim, H., Myung, H., 2014. Angular rate-constrained path planning algorithm for unmanned surface vehicles. Ocean Eng. 84, 37–44.
Kuwata, Y., Wolf, M.T., Zarzhitsky, D., Huntsberger, T.L., 2011. Safe maritime navigation with COLREGS using velocity obstacles. In: Intelligent Robots and Systems (IROS), 2011 IEEE/RSJ International Conference on. IEEE, pp. 4728–4734.
Larson, J., Bruch, M., Halterman, R., Rogers, J., Webster, R., 2008. Advances in Autonomous Obstacle Avoidance for Unmanned Surface Vehicles. Space & Naval Warfare Systems Center San Diego.
Li, B., Pang, F.W., 2013. An approach of vessel collision risk assessment based on the D–S evidence theory. Ocean Eng. 74, 16–21.
Liu, Z., Zhang, Y., Yu, X., Yuan, C., 2016. Unmanned surface vehicles: an overview of developments and challenges. Annu. Rev. Contr. 41, 71–93.
Manley, J.E., 2008. Unmanned surface vehicles, 15 years of development. In: OCEANS

2008, pp. 1–4.
Naeem, W., Irwin, G.W., Yang, A., 2012. COLREGs-based collision avoidance strategies for unmanned surface vehicles. Mechatronics 22 (6), 669–678.
Tang, P., Zhang, R., Liu, D., Huang, L., Liu, G., Deng, T., 2015. Local reactive obstacle avoidance approach for high-speed unmanned surface vehicle. Ocean Eng. 106, 128–140.
Tang, P., Zhang, R., Liu, D., Zou, Q., Shi, C., 2012. Research on near-field obstacle avoidance for unmanned surface vehicle based on heading window. In: Control and Decision Conference (CCDC), 2012 24th Chinese, pp. 1262–1267.
Wang, Y., Liang, X., Li, B., Yu, X., 2017. Research and implementation of global path planning for unmanned surface vehicle based on electronic chart. In: International Conference on Mechatronics and Intelligent Robotics, pp. 534–539.
Wang, Y., Yu, X., Liang, X., 2018. Design and implementation of global path planning system for unmanned surface vehicle among multiple task points. Int. J. Veh. Aut. Syst. 14 (1), 82–105.
Zhuang, J.Y., Wan, L., Liao, Y.L., Sun, H.B., 2011. Global path planning of unmanned surface vehicle based on electronic chart. Comp. Sci. 38 (9), 211.
Zhuang, J., Zhang, G., Su, Y., Zhang, L., Sun, H., 2013. Obstacle avoidance method for usv. J. Southeast Univ. 43, 126–130.